Evolution of a Pharaonic harbor on the Red Sea: implications for coastal response to changes in sea level and climate

Supplemental Methods

All sediment cores were topographically surveyed using a Leica TCR1103 total station with a vertical error of ± 2 cm. Eight waterline elevation measurements were collected with this same total station over three tidal cycles in January 2008 and January 2010. These data were compared to tidal predictions for El Quseir, Egypt (55 km south of Mersa / Wadi Gawasis) provided by Admiralty EasyTide (http://easytide.ukho.gov.uk/) to develop a modern mean sea level (MSL) reference elevation with an estimated vertical error of ± 5 cm. All elevations provided are calibrated to this vertical datum.

A series of wave-cut notches and an extensive 3-m wide erosional terrace were identified along the coastline and surveyed using the same instrument. The centerlines of the notches and mean elevation of the terrace surface are approximately 2.3 m and 1.8 m, respectively, above a modern +0.2 m modern notch. The modern sub-tidal coral reef platform tends to attenuate the energy of incoming waves before they strike the cliff shoreline (Trenhaile, 1987). However, in the absence of this modern terrace during the mid-Holocene, wave attenuation would have been minimized, increasing erosion potential along the cliffs, and increasing the potential height of erosional features. Hence, 1.8 m elevation is considered to be the maximum highstand given the nature of these features (Fig. 3).

Isostatic Sea-Level Model Parameters

The sea-level model requires two input components: (1) a model of late Pleistocene ice history to define the ice loading changes and the flux of ice-ocean mass exchange and (2) an earth model to compute the isostatic deformation associated with the surface water mass redistribution between ice sheets and oceans. Two ice history models are considered, one presented by Bradley et al. (2010) and the well-known ICE-5G model (e.g. Peltier, 2004). Note that the former, calibrated using Holocene sea-level data from China and the Malay-Thai Peninsula, is similar to another leading model (e.g. Lambeck and Purcell, 2005).

The viscosity structure of the earth model is one of the primary sources of uncertainty in the sea-level predictions. For this reason, a number of models were run that sampled a range of viscosity values for a standard 3-layer configuration of this parameter in a spherical earth model: an outer shell of very high viscosity with a prescribed thickness to simulate the lithosphere; two deeper regions with constant viscosity – the first from the base of the lithosphere to the 660 km seismic velocity discontinuity and the second from this depth to the core-mantle boundary at ~2900 km depth. These latter two regions are known as the upper and lower mantle, respectively. A range of values for these three Earth model parameters was considered: lithospheric thickness (46, 71, 96 and 120 km); upper mantle viscosity (3-8 × 10^{20} Pas); lower mantle viscosity (1-50 × 10^{21} Pas).

A total of 16 model runs were performed based on the above described ice and Earth model parameters. The results, shown in Fig. DR1, indicate that a subset of these results are compatible with the Holocene sea levels at Wadi Gawasis and thus support the conclusion that isostatic processes can account for the changes in sea-level observed at this locality. One of the model outputs that is compatible with the data is shown in Fig. 3 of the main text.

DATA REPOSITORY FIGURES AND TABLES

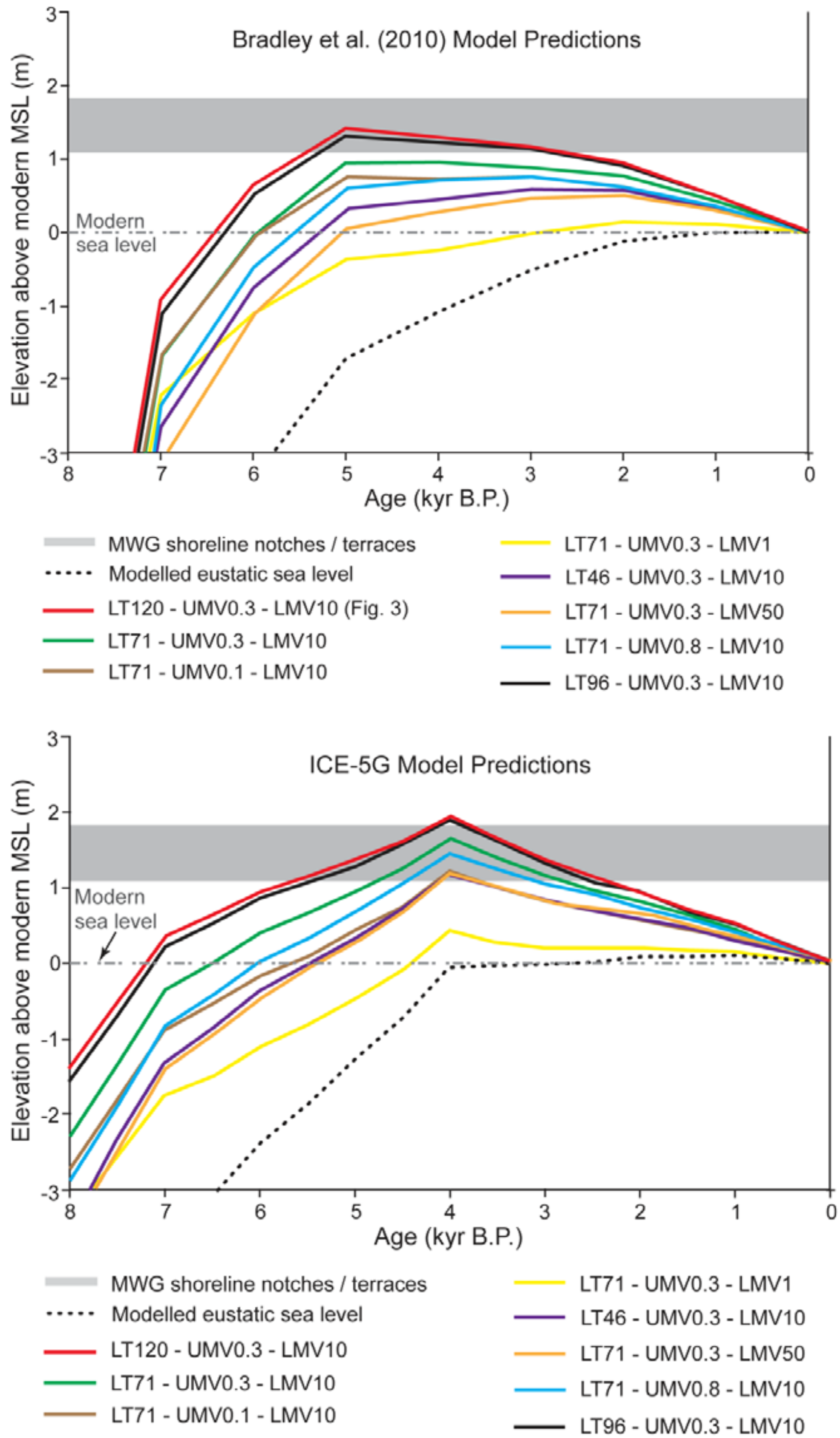

Figure DR1. Relative sea level predictions at Wadi Gawasis created using A) model of Bradley et al. (2010) and B) ICE-5G (Peltier, 2004). Eight runs were performed using each model. The parameters varied in each model run are discussed in the accompanying text. Parameters noted in key are as follows: LT – lithospheric thickness (km); UMV – upper mantle viscosity (x 10^{21} Pas); LMV – lower mantle viscosity (x 10^{21} Pas). Note that a subset of the model parameter sets considered in each run is compatible with the observed highstand amplitude of 1.1 to 1.8 m (horizontal gray box; see main text). Scales are same as those presented in Fig. 3.

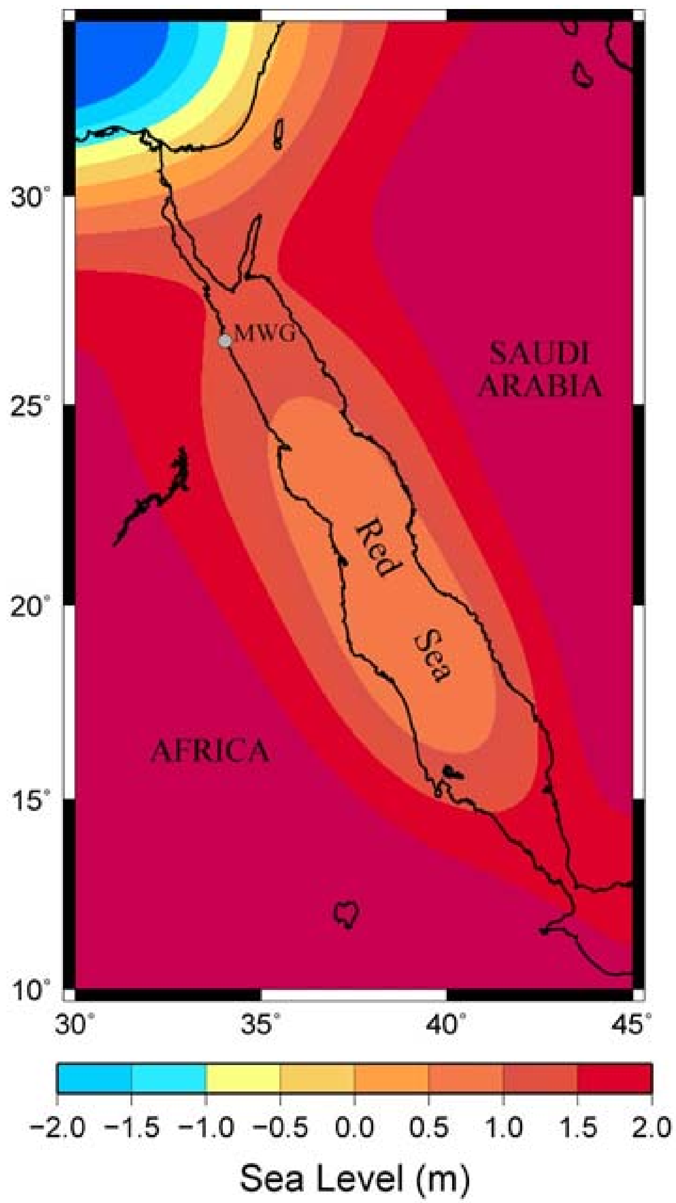

Figure DR2. Relative sea level predicted for the Red Sea region for the time 5 cal. kyr BP (i.e. the time of the predicted maximum in Holocene sea levels for the study area). This prediction is based on one of the model runs that compared well with the observations (Bradley et al. [2010] ice model with LT120–UMV0.3–LMV10 Earth model; shown in Fig. 3 and Fig. DR1a). The spatial variation in the predicted signal is dominated by the influence of ocean loading following the large (order 100 m) rise in global mean sea level accompanying the main phase of deglaciation from ~21-7 cal. kyr BP. The isostatic response of the solid Earth to this loading causes a broad and subtle uplift of the land between the Mediterranean Sea and the Indian Ocean, which contributes to the fall in sea levels observed in this region during the mid-to-late Holocene. Note that the sea-level rise within the Red Sea following the last glacial maximum also contributes to this water loading signal (in this case the loading acts to cause a subsidence along the banks of the Red Sea that reduces the amplitude of the predicted Holocene high stand). The sea-level highstand predicted by the model at Wadi Gawasis results from two processes: (i) the regional ocean loading signal (excluding the more local loading in the Red Sea) causing a land uplift and (ii) a steady fall in global ocean surface height due to an increase in ocean basin volume (so-called 'ocean syphoning' – see, for example, Mitrovica and Milne (2002)).

Table DR1. Recorded evidence of a mid-Holocene highstand along the Red Sea Coast of Egypt. Records are presented in order of descending latitude. Side IDs correspond to locations noted in Fig. 1A. Elevations, dates, and date ranges are presented when reported. Where applicable, raw radiocarbon dates have been calibrated using Marine09 (Reimer et al., 2009) and with local correction calibrated to reported data from Hurghada: $\delta R = 150$ yrs; δR uncertainty = 45 years and are reported with standard errors (s.e.m).

TABLE DR1. RED SEA HOLOCENE HIGHSTAND RECORDS

Site ID	Site Name	North Lat.	East Long.	Sea Level Marker	Elevation Above Modern MSL	Reported Radiocarbon Age (BP)	Calibrated (1 sigma) Radiocarbon Age OR U/Th Age (BP)	Citation
1	Eilat, Israel, Gulf of Aqaba	29° 32'	34° 57'	Coral terrace	-1 m to 1 m	4770 ± 140	4827 ± 211	Friedman, 1965
2	Eilat, Israel, Gulf of Aqaba	29° 31'	34° 56'	Emergent reef terrace	2 m	4450 - 5750	4423 - 6017	Moustafa et al., 2000
3	Eilat, Israel, Gulf of Aqaba	29° 31'	34° 56'	Coral terrace	1 m	N/A	5380 ± 50	Shaked et al., 2004
4	Eilat, Israel, Gulf of Aqaba	29° 31'	34° 56'	Coral terrace	1 m	N/A	4960 ± 50	Shaked et al., 2004
5	Jordanian Coast of Gulf of Aqaba	29° 27'	34° 58'	Reef Terrace	0.45 - 0.55 m	5570 - 6210	5774 - 6480	Dullo and Montaggioni, 1998
6	Jordanian Coast of Gulf of Aqaba	29° 27'	34° 58'	Reef Terrace	1 - 2 m	Interpreted as mid-Holocene	N/A	Al-Kifaiy and Cherif, 1988; Bouchon et al., 1981
7	Umm-Sid Reef: Esh-Shaura El-Manqata, Egypt	28° 13'	34° 26'	Reef Terrace	0.5 m	Range of dates: 2500 - 6800 (mean 4885)	N/A	Gvirtzman et al., 1992; Gvirtzman, 1994
8	Umm-Sid Reef: Maria Schroeder Wreck, Egypt	28° 11'	34° 27'	Reef Terrace	0.5 m	Range of dates: 5300 - 6500 (mean 5800)	N/A	Gvirtzman et al., 1992; Gvirtzman, 1994
9	Ras Shukeir, Egypt	28° 08'	33° 14'	Coral terrace	1 m	5420 ± 350	5655 ± 410	Plaziat et al., 1998
10	Ras Dib, Egypt	28° 01'	33° 24'	Coral terrace	2 m	5740 ± 360	5978 ± 395	Plaziat et al., 1998
11	Ras Dib, Egypt	28° 01'	33° 24'	Coral terrace	2 m	5550 ± 380	5773 ± 428	Plaziat et al., 1998
12	Gebel Abu Shaar, Egypt	27° 18'	33° 45'	Shell middens	2 m	5365 - 6075	5572 - 6352	Plaziat et al., 1998
13	Hurghada, Safaga, Giftun Islands, Egypt	26° 45' to 27° 13'	33° 58' to 33° 51'	Reef terrace	0.2 - 0.45 m	3930 - 5580	3721 - 5792	Dullo and Montaggioni, 1998
14	Safaga to Ras Banas, Egypt	23° 56' to 26° 43'	35° 29' to 33° 56'	Erosional terrace	1 m	5390 - 6410	5615 - 6713	Plaziat et al., 1998
15	Wadi Ambagi, Quseir, Egypt	26° 09'	34° 15'	Fluvial terraces in wadi	1.5 m & 4 m	N/A; interpreted as Holocene	N/A	Büdel, 1952
16	Wadi Umm Gheig, Egypt	25° 43'	34° 32'	Fluvial terrace	1 - 2 m	N/A; interpreted as ~6 kya	N/A	Arvidson et al., 1994
17	Wadi Mubarak, Egypt	25° 31'	34° 39'	Fluvial / coral terrace	1 - 2 m	N/A; interpreted as ~6 kya	N/A	Arvidson et al., 1994
18	Mersa Alam North, Egypt	25° 16'	34° 46'	Coral terrace	2 m	Dated sample contaminated; not interpreted	N/A	Veeh and Giegengack, 1970
19	Wadi Seifan, Egypt	25° 06'	34° 52'	Fluvial terrace	2 - 3 m	N/A; interpreted as ~6 kya	N/A	Arvidson et al., 1994
20	Wadi Gemal, Egypt	24° 15'	35° 25'	Erosional terrace	0.5 - 1 m	7670 ± 206	7978 ± 215	Plaziat et al., 1995
21	Wadi Gemal, Egypt	24° 15'	35° 25'	Erosional terrace	1 m	5800 ± 250	4200 ± 300	Plaziat et al., 1998
22	Hamata / Wadi Lahami, Egypt	24° 13'	35° 25'	Erosional terrace	0.5 - 1 m	6410 ± 84	6722 ± 118	Plaziat et al., 1995
23	Hamata / Wadi Lahami, Egypt	24° 13'	35° 25'	Shell-rich *in situ* sand	2 m	4820 ± 220	4939 ± 300	Plaziat et al., 1998
24	Berenike, Foul Bay, Egypt	23° 55'	35° 29'	Reef terrace	1 - 2 m	5000 - 8000	5114 - 8316	Harrell, 2000

TABLE DR2. MOLLUSKS IDENTIFIED IN CORES AT MWG

Bivalvia		Gastropoda
Pocillopora sp.	*Pinna muricata*	*Conus sp.*
Anadara antiquata	*Tridacna maxima*	*Cymatium marerubrum*
Atactodea glabrata	*Conus sp.*	*Erosaria nebrites*
Azorinus coarctatus	*Cymatium marerubrum*	*Fusinus polygonoides*
Barbatia fusca	*Erosaria nebrites*	*Nassarius fenistratus*
Callista florida	*Fusinus polygonoides*	*Nassarius obvelatus*
Circe crocea	*Nassarius fenistratus*	*Natica undulata*
Diplodonta subrotunda	*Nassarius obvelatus*	*Phasianella solida*
Fulvia sp.	*Natica undulata*	*Strombus erythrinus*
Lamellolucina dentifera	*Phasianella solida*	*Turbo radiatus*
Lioconcha ornata	*Strombus erythrinus*	
Pinctada radiata	*Turbo radiatus*	

Table DR3. Primarily abundant benthic foraminifera species identified in samples collected from lagoonal sediments. Sediment samples were treated with standard sieve procedure and identified by microscope. Environmental conditions as given by Murray (1991).

TABLE DR3. ABUNDANT BENTHIC FORAMINIFERA SPECIES

Species	Lifestyle	Environmental Conditions					Notes
		Substrate	Salinity (psu)	Depth Range	Temp °C	Environment	
Elphidium craticulatum	epifaunal / free	sand; vegetation	30 - 70 ‰	0 - 8 m	temperate-warm	lagoons; shallow shelves	-
Ammonia tepida	infaunal / free	muddy sand	30 - 36 ‰	8 - 29 m	21 - 30^{o} C; warm, temperate, tropical	brackish and hypersaline lagoons; shallow shelves	-
Peneroplis planatus	epifunal, clinging	muddy; carbonate sand; seagrass	42 - 70 ‰	0 - 15 m	16 - 40^{o} C	lagoons, estuaries, innermost shelf	most common species
Peneroplis pertusus	epifunal, clinging	muddy; carbonate sand; seagrass	42 - 70 ‰	0 - 15 m	16 - 40^{o} C	lagoons, estuaries, innermost shelf	
Quinqueloculina sp.	epifuanal, epiphytic, or free	carbonate sand and mud; seagrass	37 - 70 ‰	0 - 30 m	16 - 40^{o} C	typical lagoon species; hypersaline lagoons, marine marsh and shelf	second most common species

Table DR4. Radiocarbon dates from Wadi Gawasis. All dates from inorganic carbon (mollusk shells), except where otherwise noted. All ages calibrated using Marine09 (Reimer et al., 2009) and with local correction calibrated to reported data from Hurghada: δR = 150 yrs; δR uncertainty = 45 years. Radiocarbon analysis performed either at the National Ocean Sciences Accelerator Mass Spectrometry Facility (NOSAMS) at Woods Hole Oceanographic Institution, Woods Hole, MA, USA; or at Institut français d'archéologie orientale (IFAO), Cairo, Egypt.

TABLE DR4. RESULTS OF RADIOCARBON ANALYSIS AT MWG

Identification				Calibrated Age (ys BP)		
Core	Lab ID	Elevation Above MSL (cm)	Uncalibrated Age (ys BP)	1 sigma	2 sigma	Notes
T3A5S1	NOSAMS: 65814	-59.5	4710 ± 30	4765 ± 71	6428 ± 138	
T3A6S1	NOSAMS: 65813	42.5	4550 ± 35	4542 ± 95	4572 ± 163	
T3A6S2	NOSAMS: 64703	-117.5	4610 ± 30	4643 ± 82	4650 ± 157	
T3A6S3	NOSAMS: 64704	-347.5	5920 ± 35	6201 ± 65	6155 ± 140	
T3A7S1	NOSAMS: 64705	-133.5	6160 ± 35	6419 ± 71	6428 ± 138	
T5A4S1	NOSAMS: 64706	-367.2	4960 ± 30	5115 ± 99	5097 ± 176	
T5A5S1	NOSAMS: 64707	-49.1	4080 ± 35	3906 ± 74	3920 ± 156	
T5A5S2	NOSAMS: 64708	-284.1	4850 ± 35	4920 ± 75	4968 ± 165	
T6A3S1	IFAO: 209	8.6	3411 ± 46	3094 ± 98	3094 ± 191	date questionable (young); not incorporated into analysis
T6A5S1	NOSAMS: 65815	-73.4	4340 ± 35	4205 ± 87	4258 ± 163	
T6A5S2	NOSAMS: 64709	-388.4	4980 ± 30	5134 ± 94	5118 ± 165	
T6A6S1	NOSAMS: 64710	-95.1	4970 ± 30	5126 ± 96	5110 ± 170	
T6A6S2	NOSAMS: 64711	-240.1	5910 ± 45	6188 ± 75	6144 ± 150	
T6A7S1	NOSAMS: 64712	-243.9	4540 ± 40	4529 ± 94	4567 ± 168	
T7A1S1	IFAO: 210	62.2	3884 ± 48	3661 ± 93	3655 ± 179	date questionable (young); not incorporated into analysis
T7A2S1	IFAO: 208	37.6	3455 ± 47	3154 ± 97	3143 ± 182	date questionable (young); not incorporated into analysis
T10A2S3	NOSAMS: 79326	51.5	4410 ± 35	4359 ± 85	4356 ± 168	*In situ* coral fragment collected from buried coral terrace
T11A1S2	NOSAMS: 79314	-22.7	6610 ± 30	6952 ± 81	6971 ± 160	
T11A2S1	NOSAMS: 79315	31.4	4310 ± 30	4235 ± 88	4239 ± 159	
T11A3S1	NOSAMS: 79316	-7.5	4400 ± 30	4348 ± 79	4349 ± 161	
T11A4S1	NOSAMS: 79325	36.5	4160 ± 30	4015 ± 82	4022 ± 164	
T11A5S1	NOSAMS: 79317	-11	4920 ± 30	5028 ± 105	5046 ± 186	mollusk fragment likely reworked; not incorporated into analysis
T11A7S3	NOSAMS: 79318	-231.8	6800 ± 35	7192 ± 63	7160 ± 142	
T14A1S1	NOSAMS: 79312	-15	4350 ± 45	4910 ± 51	4914 ± 72	Avicennia marina root mass
T18A8S1	NOSAMS: 79320	-65	1520 ± 25	913 ± 63	913 ± 126	
T19A1S1	NOSAMS: 79323	-103.7	4570 ± 25	4593 ± 90	4604 ± 169	
T19A2S2	NOSAMS: 79321	-16.5	4520 ± 30	4500 ± 80	4539 ± 173	
T19A3S1	NOSAMS: 79322	-127.3	6250 ± 35	6531 ± 73	6527 ± 137	
T20A1S1	NOSAMS: 79313	25.9	4500 ± 35	4485 ± 75	4508 ± 183	
T21A2S16	NOSAMS: 79319	-14.1	6650 ± 30	7014 ± 81	7009 ± 145	
T-8	NOSAMS: 79324	1.425	24700 ± 140	Invalid Calibration		mollusk collected carbonate cemented to +2 m coral terrace; contamination likely

DATA REPOSITORY REFERENCES CITED

Al-Rifaiy, I.A. and Cherif, O.H., 1988, The fossil coral reefs of Al-Aqaba, Jordan: Facies, v. 18, p. 219–230.

Arvidson, R.E., Becker, R., Shanabrook, A., Luo, W., Sturchio, N., Sultan, M., Lofty, Z., Mahmood, A.M., and El Alfy, Z., 1994, Climatic, eustatic, and tectonic controls on Quaternary deposits and landforms, Red Sea coast, Egypt: Journal of Geophysical Research, v. 99, p. 12,175–12,190, doi:10.1029/94JB00037.

Bradley, S.L., Milne, G.A., Zong, Y.-Q., Horton, B.P., 2010, Modeling sea-level data from China and the Malay-Thai Peninsula: Quaternary Science Reviews, submitted.

Büdel, J., 1952, Bericht über klimamorphologische und Eiszeitforschungen in Niederafrika (Report on the climate-geomorphological and ice age research in Lower Africa), *Erdkunde* v. 2/3.

Dullo, W.-C. and Montaggioni, L., 1998, Modern Red Sea coral reefs: a review of their morphologies and zonation, in Purser, B.H., and Bosemce, D.W.J., eds., Sedimentation and Tectonics of Rift Basins: Red Sea - Gulf of Aden: Cambridge, Chapman and Hall, p. 583-594.

Friedman, G.M., 1965, A fossil shoreline reef in the Gulf of Elat (Aqaba): Israeli Journal of Earth Sciences, v. 14, p. 86–90.

Gvirtzman, G., 1994, Fluctuations of sea level during the past 400,000 years: the records of Sinai, Egypt (northern Red Sea): Coral Reefs, v. 13, p. 203–214.

Gvirtzman, G., Kronfeld, J. and Buchbinder, B., 1992, Dated coral reefs of southern Sinai (Red Sea) and their implication to late Quaternary sea levels: Marine Geology, v. 108, p. 29–37.

Harrell, J.A., 1998, Geology, in Sidebotham, S.E., and Wendrich, W.E., eds., Berenike 1996: Report of the 1996 excavations at Berenike (Egyptian Red Sea Coast) and the survey of the Egyptian Eastern Desert: Amsterdam, CNWS, p. 121-131.

Lambeck, K., and Purcell, A., 2005, Sea-level change in the Mediterranean Sea since the LGM: model predictions for tectonically stable areas: Quaternary Science Reviews, v. 24, p. 1969-1988.

Mitrovica, J.X. and Milne, G.A., 2002, On the origin of late Holocene sea-level highstands within equatorial ocean basins: Quaternary Science Reviews, v. 21, p. 2179-2190.

Moustafa, Y.A., Patzold, J., Loya, Y., and Wefer, G., 2000, Mid-Holocene stable isotope record of corals from the northern Red Sea: International Journal of Earth Sciences, v. 88, P. 742-751.

Murray, J.W., 1991, Ecology and palaeoecology of benthic foraminifera: New York, Longman, 397 p.

Peltier, W.R., 2004, Global glacial isostasy and the surface of the ice-age Earth: the ICE-5G (VM2) model and GRACE: Annual Review of Earth and Planetary Sciences, v. 32, p. 111-149.

Plaziat, J.-C., Baltzer, F., Choukri, A., Conchon, O., Freytet, P., Orszag-Sperber, F., Purser, B., Raguideau, A., and Reyss, J.-L., 1995, Quaternary changes in the Egyptian shoreline of the Northwestern Red Sea and Gulf of Suez: Quaternary International, v. 29/30, p. 11-22.

Plaziat, J.-C., Baltzer, F., Choukri, A., Conchon, O., Freylet, P., Orszag-Sperber, F., Raguideau, A., and Reyss, J.-L., 1998, Quaternary marine and continental sedimentation in the northern Red Sea and Gulf of Suez (Egyptian coast): influences of rift tectonics, climatic changes and sea-level flucuations, in Purser, B.H., and Bosemce, D.W.J., eds., Sedimentation and Tectonics of Rift Basins: Red Sea - Gulf of Aden: Cambridge, Chapman and Hall, p. 537-573.

Reimer, P.J., Baillie, M.G.L., Bard, E., Bayliss, A., Beck, J.W., Blackwell, P.G., Ramsey, C.B., Buck, C.E., Burr, G.S., Edwards, R.L., Friedrich, M., Grootes, P.M., Guilderson, T.P., Hajdas, I., Heaton, T.J., Hogg, A.G., Hughen, K.A., Kaiser, K.F., Kromer, B., McCormac, F.G., Manning, S.W., Reimer, R.W., Richards, D.A., Southon, J.R., Talamo, S., Turney, C.S.M., van der Plicht, J., and Weyhenmeyer, C.E., 2009, IntCal09 and Marine09 Radiocarbon Age Calibration Curves, 0–50,000 Years cal BP: Radiocarbon v. 51, p. 1111–1150.

Shaked, Y., Agnon, A., Lazar, B., Marcio, S., Avner, U., and Stein, M., 2004, Large earthquakes kill coral reefs at the north-west Gulf of Aqaba: Terra Nova, v. 16, p. 133-138.

Trenhaile, A.S., 1987, The Geomorphology of Rock Coasts: New York, Oxford University Press, 394 p.

Veeh, H.H. and Giegengack, R., 1970, Uranium-series ages of corals from the Red Sea: Nature, V. 226, p. 155-156.